Antitumor effects of aconitine in A2780 cells via estrogen receptor β-mediated apoptosis, DNA damage and migration

XIUYING WANG[1], YUANYUAN LIN[2] and YI ZHENG[3]

[1]Pharmaceutical Preparation Section, People's Hospital of Weifang High-tech Zone, Weifang, Shangdong 261205; [2]Department of Nursing, Weifang Hospital of Traditional Chinese Medicine, Weifang, Shandong 261031; [3]Department of Medical Oncology, Affiliated Hospital of Weifang Medical University, Weifang, Shandong 261041, P.R. China

Received April 24, 2019; Accepted March 31, 2020

DOI: 10.3892/mmr.2020.11322

Abstract. Ovarian cancer (OVCA) is the deadliest type of malignant gynecological disease, and previous studies have demonstrated that estrogen receptor β (ERβ) serves important roles in this disease. Aconitine, a toxin produced by the Aconitum plant, displays potent effects against cancers. The aim of the study was to investigate the pharmacological activities and mechanisms of aconitum on OVCA. In the present study, the activity of aconitine in the human OVCA A2780 cell line was investigated. The results revealed that aconitine suppressed cell viability, colony formation and motility. Terminal deoxynucleotidyl-transferase-mediated dUTP nick end labeling, mitochondria membrane potential and comet assays showed that aconitine induced mitochondria apoptosis and DNA damage in A2780 cells. Investigation of the mechanism revealed that a high expression of ERβ and prolyl hydroxylase 2 was detected after aconitine treatment, and aconitine significantly suppressed the expression of vascular endothelial growth factor and hypoxia-inducible factor 1α to activate ERβ signaling. Moreover, the expression levels of p53, Bax, apoptotic peptidase activating factor 1, cytochrome C, cleaved caspase-3/9 and cleaved poly (ADP-ribose) polymerase were upregulated, and the expression levels of Bcl-2, Bcl-xl and phosphorylated ATM serine/threonine kinase were downregulated by aconitine. Interestingly, aconitine also markedly downregulated the expression of matrix metalloproteinase 2 (MMP2) and MMP9, which are associated with tumor invasion. In addition, a molecular docking assay revealed that aconitine exerted strong affinity towards ERβ mainly through hydrogen bonding and hydrophobic effects. Collectively, these results suggested that aconitine suppressed OVCA cell growth by adjusting ERβ-mediated apoptosis, DNA damage and migration, which should be considered a potential option for the future treatment of OVCA.

Correspondence to: Dr Yi Zheng, Department of Medical Oncology, Affiliated Hospital of Weifang Medical University, 2428 Yuhe Road, Weifang, Shandong 261041, P.R. China
E-mail: zhengyizl0304@126.com

Key words: ovarian cancer, aconitine, estrogen receptor β

Introduction

Ovarian cancer (OVCA) has a high mortality rate of 30-50%, is the fifth most common type of cancer worldwide, and is also the cause of the majority of cancer-related mortality in women (1,2). Chemotherapy is the standard treatment for OVCA; however, 70% of patients with terminal cancer experience chemoresistance or recurrence within 15 months of treatment (3). Currently, chemotherapy is extensively used to treat OVCA. However, certain antitumor drugs, including cisplatin and sorafenib, can have serious side effects that limit their clinical applications (4,5). Thus, exploration of new drugs or active compounds for the therapy of OVCA is urgent.

Steroid hormones are very important for the development of OVCA, as the progesterone receptor (PR) and estrogen receptor (ER) have been confirmed to be associated with survival rate and prognosis of patients with cancer (6,7). The ERs, including the two ER subtypes ERα and ERβ, have been widely studied in OVCA (8,9). The two ER subtypes have different specificity in ligand binding, with opposing functions in cell growth in some types of cancer (10,11). ERα and a gene target of estrogen signaling, PR, are prognostic biomarkers in OVCA. It has been elucidated that 40-60% of OVCA cases express ERα, but only a small proportion of patients respond to ER antagonist tamoxifen therapy (12). Previous studies have suggested, in contrast to ERα, that ERβ expression is significantly lower in malignant tissue compared with normal tissue, and its expression is a useful predictor for disease-free survival and overall survival (13,14). Previous studies have indicated that the expression level of ERβ is decreased in localized prostate cancer suggesting that ERβ may be a suppressor gene (14). Functionally, exogenous expression of ERβ in OVCA can inhibit cell proliferation and increase cell apoptosis via promoting the degradation of hypoxia-inducible factor (HIF)-1α (15). Vascular endothelial growth factor A (VEGFA) signaling was inhibited by low levels of HIF-1α, which is a critical component in preventing apoptosis and motility of tumor cells. In short, the activation of ERβ expression may be

an effective target for the exploration of compounds to treat OVCA (16,17).

Traditional Chinese medicines have been used to treat cancer for thousands of years, using a large collection of biologically active products (18-21). Natural compounds from medicinal plants, including dioscin and berberine, have potent effects against various types of cancer (22-28); it is reported that berberine inhibited human cervical carcinoma HeLa cells and dioscin induced DNA damage and activated mitochondrial signal pathway in human A549, NCI-H446 and NCI-H460 cancer cell lines (29,30). Additionally, some natural products, including genistein and daidzein, have been reported to inhibit migration, invasion and proliferation of OVCA cells (31). Thus, exploration of effective natural products from medicinal plants is a reasonable approach to treat OVCA.

Aconitine (Fig. 1A), also known as monkshood or devil's helmet, is a type of toxin produced by the Aconitum plant that has been used as a traditional medicine in China due to its analgesic and anti-inflammatory effects (32). A previous study has indicated that aconitine can induce apoptosis in human pancreatic cancer cells via the NF-κB signaling pathway (33). In addition, aconitine can induce apoptosis in human cervical carcinoma HeLa cells by adjusting endoplasmic reticulum stress signaling (34). However, no previous studies have reported the effects and molecular mechanisms of aconitine against OVCA, and therefore, the aim of the current study was to investigate this compound in OVCA cells *in vitro*.

Materials and methods

Chemicals and reagents. Aconitine was obtained from the Chengdu Research Institute of Biology of the Chinese Academy of Sciences. MTT was obtained from Roche Diagnostics. Protein Extraction kit (cat. no. KGP250), penicillin and streptomycin combination were purchased from Nanjing KeyGen Biotech Co., Ltd. Dulbecco's modified Eagle's medium (DMEM) and fetal bovine serum (FBS; cat. no. 10099-141) were purchased from Gibco; Thermo Fisher Scientific, Inc. 4',6'-Diamidino-2-phenylindole (DAPI) was purchased from Sigma-Aldrich; Merck KGaA. Comet assay kit (cat. no. 4250) was purchased from Cell Biolabs, Inc. The TUNEL assay kit (cat. no. FA201) was purchased from Beijing Transgen Biotech Co., Ltd. JC-1 mitochondrial membrane potential assay kits (cat. no. C2006) were obtained from Beyotime Institute of Biotechnology. Primary and secondary antibodies were purchased from ProteinTech Group or BIOSS and are presented in Table I. BSA blocking buffer was purchased from Beijing Solarbio Science & Technology Co, Ltd (cat. no. SW3015).

Cell lines and culture. The human OVCA cell lines, A2780 and normal ovarian cell IOSE80, were purchased from Wuhan Boster Biological Technology, Ltd. A2780 and IOSE80 cells were cultured in DMEM medium in the presence of 10% FBS, supplemented with 100 U/ml penicillin and 100 g/ml streptomycin, and cultured in a humidified 5% (v/v) atmosphere of CO_2 in an incubator at 37˚C.

Cell viability assay. A cell viability assay was performed using MTT. Cells were plated into 96-well plates ($5x10^4$ cells/well) and incubated at 37˚C overnight. In the present study the concentrations of aconitine used in the cell viability assay were 10, 50, 100, 200, 400, 800 and 1,000 μg/ml. $5x10^4$ cells/well A2780 cells and normal ovarian IOSE80 cells were then treated with various concentrations of aconitine (10, 50, 100, 200, 400, 800 and 1,000 μg/ml) and positive control cisplatin (1, 5, 25, 50 and 100 μg/ml) for different exposure times of 6, 12 and 24 h. Next, 10 μl of MTT (5 mg/ml) was added to each well and incubated for a further 4 h at 37˚C. Following this, 150 μl DMSO was added to dissolve formazan crystals, the absorbance was read at 490 nm using a microplate reader (Thermo Fisher Scientific, Inc.), and cell morphology was obtained with a phase-contrast microscope (Nikon Corporation).

Plate colony-forming assay. A2780 cells in 6-well plates at a density of 500 cells per well were treated with aconitine (0, 100, 200 and 400 μg/ml) once every 3 days. The treated cells were incubated at 37˚C for 10 days, and the medium was changed every day. Finally, the cells were stained with crystal violet at room temperature for 30 min and then, colonies containing >50 cells were counted. The colony formation numbers were analyzed using ImageJ software 1.3 (National Institutes of Health).

Wound healing assay. A2780 cells ($2x10^5$ cells/well) were cultured for 12 h at 37˚C, then the cells were scratched with a sterile micro-pipette tip and washed with PBS to remove cell debris in the serum-free medium. After cells were treated with aconitine (0, 25, 50 and 100 μg/ml) at 37˚C for 24 h, the non-adherent cells were washed away with PBS and the migration distance was taken and analyzed using ImageJ software 1.3. The morphology of the cells was obtained by a phase contrast microscope (Nikon Corporation) at x200 magnification.

Transwell migration assay. The migration potential of A2780 cells was assessed using Transwell chambers (8 μm pore; Corning Inc.). A total of $6x10^4$ cells in serum-free medium (200 μl) were added to the upper chamber, while the lower chamber was filled with 500 μl medium containing 20% FBS. After incubation with aconitine (0, 25, 50 and 100 μg/ml) in the upper chamber for 12 h at 37˚C, the cells were fixed with methanol for 30 min and stained with crystal violet for 20 min at room temperature. Finally, cells were imaged under an inverted phase-contrast microscope and ImageJ software 1.3 (National Institutes of Health) was used for quantification.

Terminal deoxynucleotidyl-transferase-mediated dUTP nick end labeling (TUNEL) assay. Early and late apoptosis apoptosis was determined using the TransDetect® *In Situ* Fluorescein TUNEL Cell Apoptosis Detection kit according to the manufacturer's protocols. The solution of 10% green fluorescein labeled dUTP was added to $6x10^4$ A2780 cells that were incubated at 37˚C for 1 h. Next, the samples were washed with cell permeable fluid and neutral gum sealer was used as the mounting medium. Images of five random fields of view were captured using a fluorescence microscope (Olympus Corporation) at x200 magnification.

Mitochondrial membrane potential assay. $6x10^4$ A2780 cells were incubated with JC-1 dye working fluid in an incubator

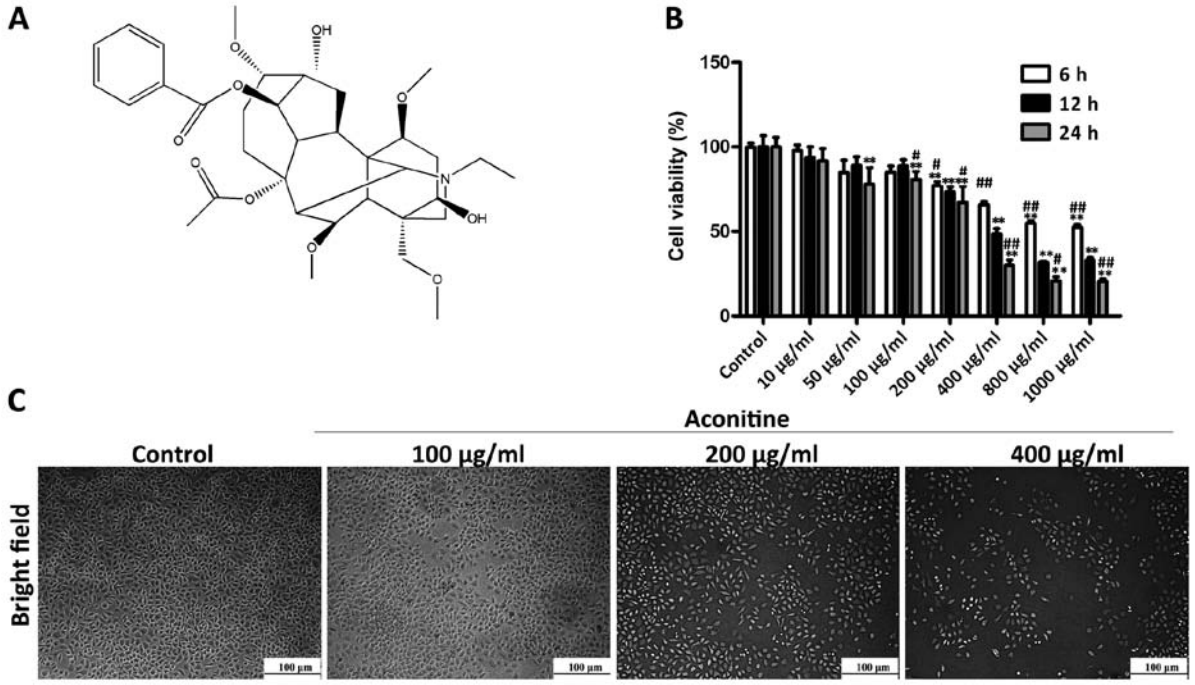

Figure 1. Effects of aconitine on the viability of A2780 cells. (A) Chemical structure of aconitine. (B) Effects of aconitine on the viability of A2780 cells detected by MTT assay. (C) Morphological changes of the cells treated by different concentrations of aconitine (100, 200 and 400 μg/ml) for 24 h by bright-field images obtained using a light microscope. Scale bar, 100 μm. Data are presented as mean ± SD of five independent experiments. *P<0.05, **P<0.01 vs. corresponding control group at 6, 12 and 24 h. $^{\#}$P<0.05, $^{\#\#}$P<0.01 vs. corresponding treatment group at 12 h.

for 20 min at 37˚C. After washing twice with a dye buffer, the JC-1 levels were determined by fluorescence microscope at x200 magnification.

Comet assay. The culture and treatment of A2780 cells were the same as TUNEL staining. After the treatment with different concentrations of aconitine (100, 200 and 400 μg/ml) for 24 h, the extent of DNA damage was determined by the Comet assay kit (Cell Biolabs, Inc.), according to the manufacturer's instructions. Images were taken using a fluorescence microscope and the Comet Assay Software Project (CASP) 1.2.2 (CaspLab) was used to analyze 50 cells from each of the 2 replicate slides.

Immunofluorescence assay. A total of 6x10^4 A2780 cells were incubated with DMEM in a 6-well plate at 37˚C overnight. After pretreatment, the cells were washed with PBS, fixed with 4% paraformaldehyde for 15 min at 4˚C, then washed with PBS and permeabilized with 0.2% Triton-100 for 8 min at 4˚C. Non-specific binding was blocked by incubating cells in 3% BSA for 1 h at 37˚C and then cells were incubated with rabbit anti-ERβ primary antibody (1:500) at 4˚C overnight. After washing with PBS three times, the samples were incubated with a FITC-conjugated goat anti-rabbit IgG (1:2,000) for 1 h at room temperature, and then DAPI (5 μg/ml) was used to stain the cell nucleus for 10 min at 4˚C. Images were captured using a fluorescence microscope at x200 magnification. The cells in five randomly selected high-power fields were counted under the fluorescence microscope and relative fluorescence intensity (total fluorescence intensity/area) represented the fluorescence intensity of the positive cells compared with the control group.

Western blotting. Total protein samples from A2780 cells were extracted by cell lysis buffer containing 1% phenylmeth-anesulfonyl fluoride (PMSF). A bicinchoninic acid assay was performed to determine the protein content. The samples (50 ng/μl) were separated by SDS-PAGE on 10-15% gels and transferred to a PVDF membrane. Following this, the membranes were incubated with primary antibodies (listed in Table I) at 4˚C overnight. The membranes were then incubated with horseradish peroxidase-conjugated secondary antibody (1:2,000) for 2 h at room temperature. Subsequently, protein bands were detected using an enhanced chemiluminescence system and ChemiDoc XRS (Bio-Rad Laboratories, Inc.). Intensity values of the relative expression levels of the proteins were normalized to GAPDH.

Molecular docking assay. The 3-dimensional (3D) structure of aconitine was optimized using the Gaussian 09 program (35) with the level of B3LYP/6-31G (36,37). The Protein Data Bank (PDB) files of aconitine were produced using PRODRG Server and the crystal structure of ERβ (PDB-code, 4GV1) was downloaded from RCSB Protein Data Bank (38). The docking studies on the proteins ERβ (PDB, 2YLY) and ligand aconitine were performed with the AutoDock 4.2 software (Aka Olson Laboratory), whose process mainly involves the removal of crystal water, ions and non-standard amino-acid residues. The binding free energy and the actions of hydrogen bonds, hydrophobic and electrostatic, were analyzed. Following the requirements of the docking study, ions, water molecules and non-standard amino acid residues were removed from the proteins. For the docking case, the model with the lowest energy was selected as the binding mode for analysis.

Table I. Antibodies used in the present study.

Antibody	Source	Dilution	Company	Catalog number
ERβ	Rabbit	1:1,000	ProteinTech Group, Inc.	21244-1-AP
VEGF-A	Rabbit	1:1,000	ProteinTech Group, Inc.	19003-1-AP
HIF-α	Rabbit	1:500	ProteinTech Group, Inc.	20960-1-AP
PHD2	Rabbit	1:500	ProteinTech Group, Inc.	19886-1-AP
p53	Rabbit	1:1,000	ProteinTech Group, Inc.	10442-1-AP
Bax	Rabbit	1:1,000	ProteinTech Group, Inc.	50599-2-Ig
Bcl-2	Rabbit	1:1,000	ProteinTech Group, Inc.	60178-1-Ig
Bcl-xl	Rabbit	1:1,000	ProteinTech Group, Inc.	26967-1-AP
Apaf-1	Rabbit	1:1,000	ProteinTech Group, Inc.	21710-1-AP
Cleaved Caspase-3	Rabbit	1:1,000	ProteinTech Group, Inc.	19677-1-AP
Cleaved Caspase-9	Rabbit	1:1,000	ProteinTech Group, Inc.	10380-1-AP
Cleaved PARP	Rabbit	1:1,000	ProteinTech Group, Inc.	13371-1-AP
Cytochrome C	Rabbit	1:1,000	ProteinTech Group, Inc.	66264-1-Ig
MMP2	Rabbit	1:1,000	ProteinTech Group, Inc.	10373-2-AP
MMP9	Rabbit	1:1,000	ProteinTech Group, Inc.	10375-2-AP
ATM	Rabbit	1:500	BIOSS	bs-1370R
p-ATM	Rabbit	1:500	BIOSS	bs-12545R
Coralite 594-conjugated AffiniPure Goat Anti-Rabbit IgG (H+L)	Rabbit	1:2,000	ProteinTech Group, Inc.	SA00013-4
Horse radish peroxide-conjugated AffiniPure Goat Anti-Rabbit IgG (H+L)	Rabbit	1:2,000	Proteintech Group, Inc.	SA00001-2

ERβ, estrogen receptor β; VEGF, vascular endothelial growth factor A; HIF-α, hypoxia-inducible factor; PHD2, prolyl hydroxylase domain-containing protein 2; MMP, matrix metalloproteinase; ATM, ATM serine/threonine kinase; p-, phosphorylated; Apaf-1, apoptotic peptidase activating factor 1; PARP, poly (ADP-ribose) polymerase.

Statistical analysis. All data are presented as mean ± SD. Statistical analysis was performed using GraphPad Prism 5.0 software (GraphPad Software, Inc.). Comparisons between two groups were performed using unpaired Student's t-test, and one-way or two-way ANOVA was followed by Bonferroni's post hoc to analyze multiple comparisons. $P<0.05$ was considered to indicate a statistically significant difference.

Results

Cytotoxicity of aconitine in A2780 cells. The MTT results presented in Fig. 1B show that aconitine treatment at the concentrations of 100, 200 and 400 μg/ml for 24 h significantly decreased cell viability to 85, 68 and 33%, respectively, compared with the control group, while effects of positive control cisplatin on the viability of A2780 cells were detected for 24 h in Fig. S1A. However, aconitine did not significantly inhibit the growth of a normal ovarian cell line (Fig. S1B). For subsequent experiments, the cells were exposed to 100, 200 or 400 μg/ml aconitine for 24 h. As shown in Fig. 1C, bright-field images suggested that cell death was induced by aconitine.

Effects of aconitine on proliferation, invasion and migration of A2780 cells. As shown in Fig. 2A, aconitine (100, 200 and 400 μg/ml) significantly decreased colony formation in A2780 cells. In addition, only low concentrations of aconitine were needed to suppress the invasive and migratory capabilities of A2780 cells compared with the control group, as demonstrated by migration and invasion assays (Fig. 2B) which excluded the influence of aconitine-induced reduction of cell viability to the experimental results of cell migration and invasion (29). These results suggested that aconitine significantly inhibited the proliferation, migration and invasion of A2780 cells (Fig. 2B).

Aconitine induces apoptosis and DNA damage in A2780 cells. To investigate the effect of aconitine on cell apoptosis, apoptosis was measured by TUNEL assay and flow cytometry. As presented in Fig. 3A, TUNEL-positive cells and apoptotic rates were significantly increased by aconitine. In addition, the results of jc-1 stain demonstrated that the intensities of red orange fluorescence in aconitine-treated groups were significantly decreased and the intensities of green fluorescence were increased compared with the control group, suggesting that aconitine increased mitochondrial membrane potential to induce mitochondria injury (Fig. 3B). In a comet assay, aconitine decreased the contents of head DNA and increased the length of DNA migration smear (comet tail) compared with the control group (Fig. 3B).

Aconitine activates the expression of ERβ in vitro. To investigate the impact of aconitine on ERβ signaling, A2780 cells

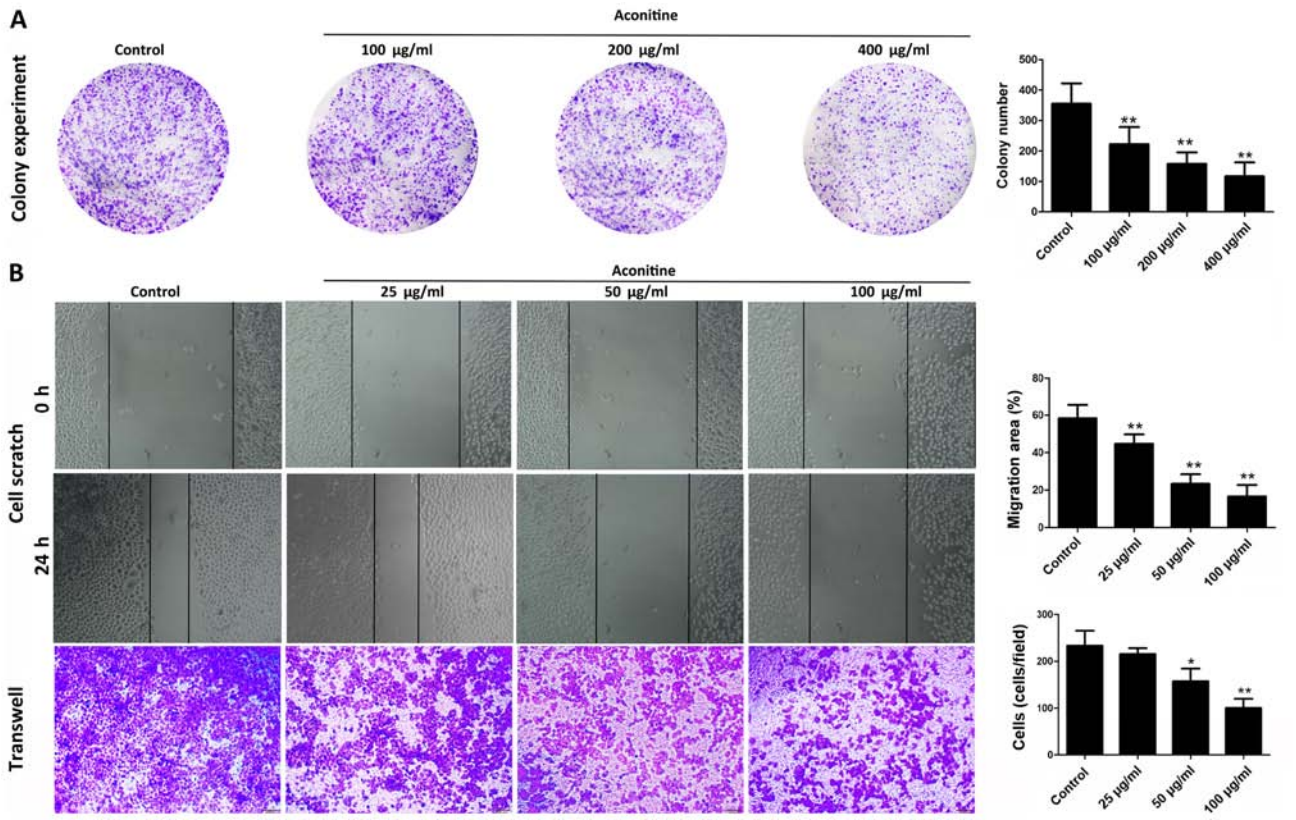

Figure 2. Aconitine inhibits colony formation and motility of A2780 cells. (A) Effects of aconitine (100, 200 and 400 μg/ml) for 24 h on colony formation in A2780 cells. (B) Effects of aconitine (25, 50 and 100 μg/ml) for 24 h on migratory and invasive properties of A2780 cells, invasion was measured in Transwell plates, and the effect of aconitine on cell migration was measured by wound-healing assay. The migration distance of A2780 cells in each concentration of aconitine was calculated as the width at 0 h minus the width at 24 h. Data are presented as the mean ± SD of three independent experiments. *P<0.05, **P<0.01 vs. control group.

were treated with different concentrations of aconitine and the expression levels of ERβ were assessed by immunofluorescence. The results presented in Fig. 4A and C indicated that, compared with the control group, the ERβ fluorescent intensity was significantly increased. In addition, the western blot analysis results in Fig. 4B indicated that aconitine significantly upregulated the expression of ERβ, and significantly downregulated the expression of VEGF compared with the control group.

Aconitine activates ERβ signaling and inhibits expression of matrix metalloproteinase (MMP) 2/9 and phosphorylated ATM serine/threonine kinase (p-ATM). As presented in Fig. 5A, western blot analysis revealed that expression of prolyl hydroxylase domain-containing protein 2 (PHD2) was significantly upregulated, and that expression of HIF-1α was markedly downregulated by aconitine compared with the control group. These results suggested that aconitine inhibited the VEGF signaling pathway by activating ERβ. Furthermore, compared with the control group, aconitine significantly increased the expression of p53 and inhibited the expression of MMP2, MMP9 and p-ATM (Fig. 5B-C).

Aconitine induces the expression of proteins associated with the mitochondria-associated apoptosis pathway. As shown in Fig. 6, compared with the control group, aconitine significantly upregulated the levels of cleaved poly (ADP-ribose) polymerase (PARP), cleaved caspase-3/9 and Bax, and downregulated the expression of Bcl-2 and Bcl-xl in A2780 cells. In addition, the expression of apoptotic peptidase activating factor 1 (Apaf-1) and cytochrome C were significantly increased by the compound.

Aconitine directly targets ERβ. A molecular docking assay was performed on ERβ to investigate the target of aconitine against OVCA. The 3D structure of aconitine and the crystal structure of ERβ (PDB ID, 2YLY) are shown in Fig. 7A and B, and the binding mode of aconitine and ERβ is shown in Fig. 7C. By molecular docking, the binding energy of aconitine towards ERβ was found to be -6.5 kcal/mol. In addition, the hydrogen bonding model of aconitine and the ERβ structure are presented in Fig. 7D, and the analyses of hydrogen bonding and hydrophobic effects showed that the amino acid residues involved in the formation of hydrogen bonds included glutamic-474 (Glu-474), asparagine-470 (Asn-470) and Glu-332 (Glu-332).

The hydrophobic bond formation of aconitine-ERβ bonding and the hydrophobic residues within the ERβ active site involves methionine-473, lysine-471, Glu-474, histidine-467, serine-333, arginine-466, alanine-497, Asn-496 and leucine-477, which further strengthens the binding of aconitine to ERβ. From the docking results, due to the strong hydrogen bonding, hydrophobic effects and electrostatic interactions, aconitine with lower binding energy possessed powerful affinity towards ERβ.

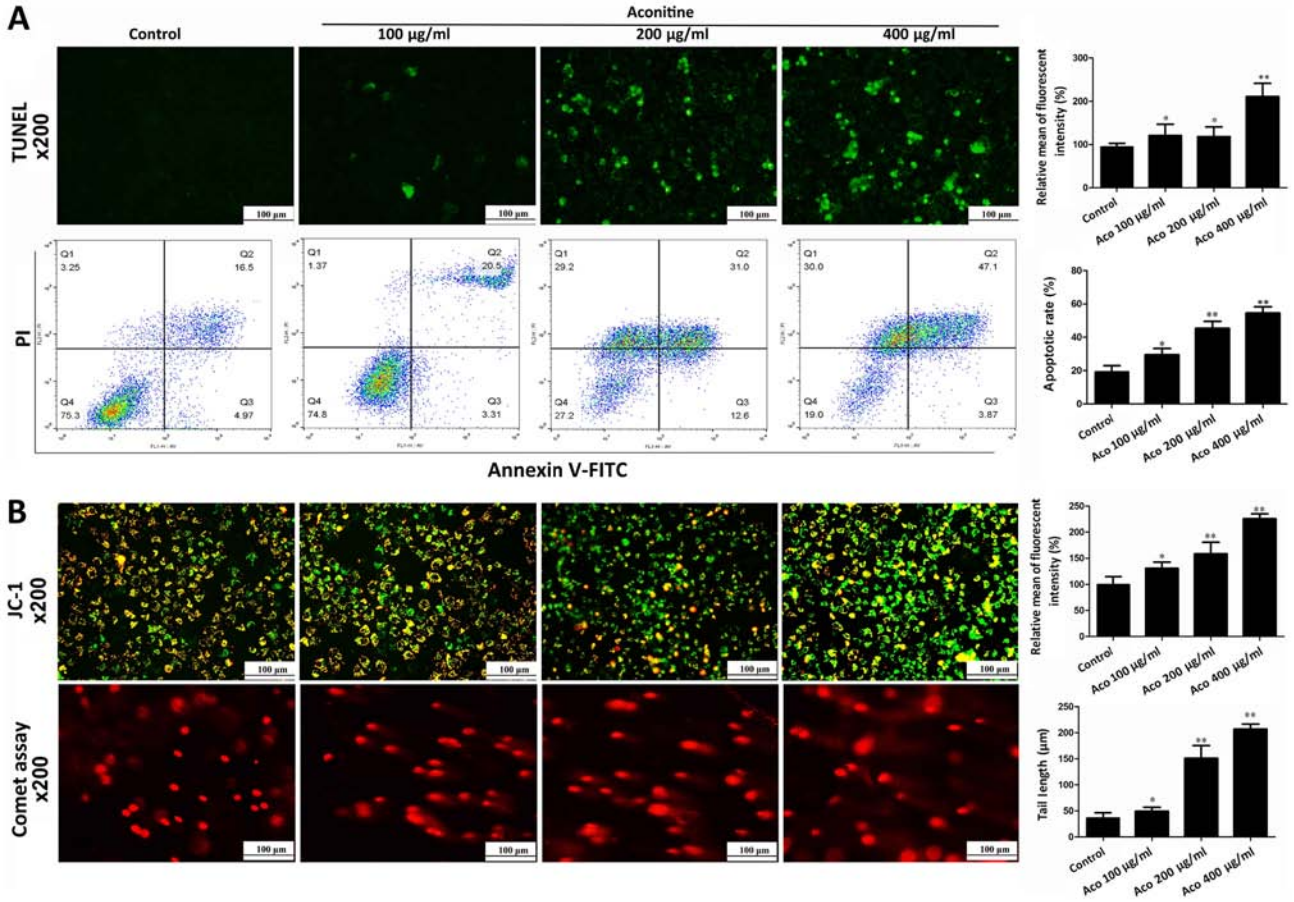

Figure 3. Aconitine induces apoptosis and DNA damage, and decreases mitochondrial membrane of A2780 cells. (A) Effects of aconitine on apoptosis measured by TUNEL and flow cytometry assays. (B) Effects of aconitine on DNA damage and mitochondria membrane potential. Scale bar, 100 μm. Data are presented as mean ± SD of three independent experiments. *P<0.05, **P<0.01 vs. control group. Aco, aconitine; PI, propidium iodide.

Discussion

OVCA is one of the most prevalent gynecological malignancies, with a global fatality rate of 6.2% (39). Although >70% of patients with OVCA can be effectively treated with surgery, novel and more effective drug interventions are needed due to the serious side effects of chemotherapy and low overall cure rates (40). As an active ingredient in the Aconitum plant, aconitine has been reported to interact with voltage-dependent sodium channels of excitable tissue cell membranes and can be metabolized by cytochrome P450 (41). However, few studies have reported the effects of aconitine on tumorigenesis. Therefore, the inhibitory effect of aconitine on human ovarian A2780 cells was investigated in the current study. The results suggested that cell viability and colony formation of A2780 cells were significantly suppressed by aconitine. In addition, low concentrations of aconitine (25, 50 and 100 μg/ml) were found to significantly suppress the invasive and migratory capabilities of A2780 cells, although these concentrations did not induce significant rates of cell death according to the MTT results. These results suggested that aconitine may have potential as a treatment for OVCA. Cytogenetic analysis showed that A2780 cells had a greater genomic stability in comparison with SKOV3 cells (42). On the other hand, A2780 cells undergo apoptosis and consequently cell death more easily than SKOV3. Thus, A2780 was chosen as the cell line to confirm the research data.

The collapse of mitochondrial function, including changes to the mitochondrial membrane potential and permeability, are associated with apoptosis (43). A previous study reported that the collapse of the mitochondrial membrane potential is an early step in apoptosis. Also, DNA fragmentation is one of the most typical phenomena of apoptosis (44). In the present study, aconitine was found to cause the disintegration of the mitochondrial membrane potential and the transformation of mitochondrial permeability. The comet assay showed that after aconitine treatment, the DNA content was transferred to the tail of the comet, suggesting that aconitine treatment induced DNA damage. In addition, the number of apoptotic cells was increased by aconitine treatment. These data showed that aconitine had potent activity against OVCA cells *in vitro* by regulating DNA damage and mitochondrial apoptosis.

A wide range of expression levels of steroid hormone receptors has been reported in OVCA. In previous years, ERβ targeting has attracted attention in various types of tumors due to its anticancer effect (45). With the decreased expression of ERβ in breast, colon and prostate cancer, the receptor is considered to be a tumor suppressor factor (6,7,46). ERβ has the highest expression in normal ovarian tissues, and this is decreased during dedifferentiation (47). A previous study has

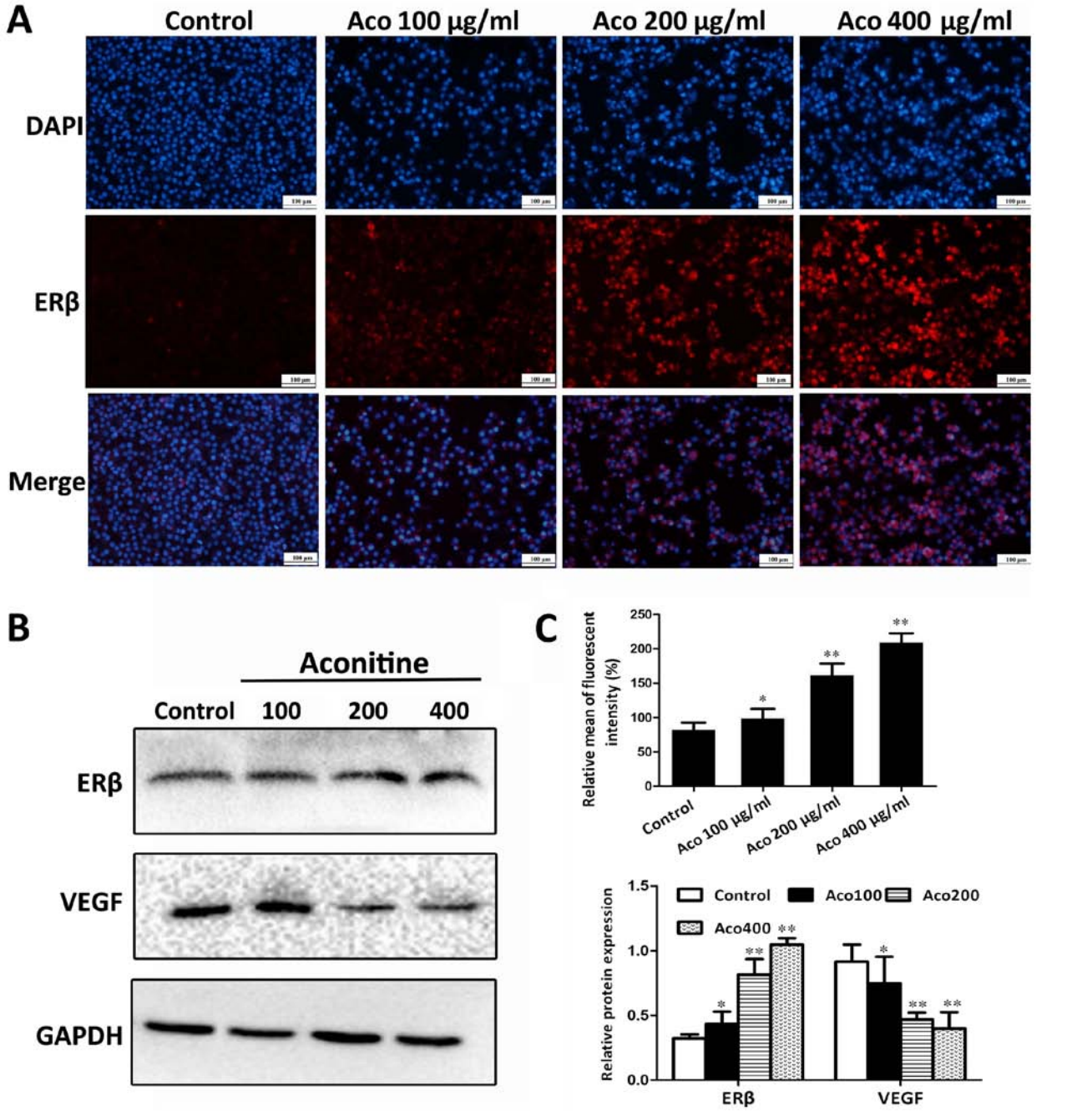

Figure 4. Effects of aconitine on the expression levels of ERβ. (A) Effects of aconitine on the expression levels of ERβ by immunofluorescence. (B) Effects of aconitine on the expression levels of ERβ and VEFG and (C) statistical analyses of fluorescence intensity of the positive cells compared with the control group. Scale bar, 100 μm. Data are presented as mean ± SD of three independent experiments. *P<0.05, **P<0.01 vs. control group. Aco, aconitine; ERβ, estrogen receptor β; VEGF, vascular endothelial growth factor A.

demonstrated that the decrease of ERβ can stabilize HIF-1α, which can lead to autocrine VEGF signaling by decreasing the enzyme activity of PHD2, the key hydroxylase of HIF-1α which suggested that ERβ is an important part of this process in tumorigenesis (14). As HIF-1α/VEGF signaling is an important regulator of cell migration and apoptosis, apoptosis can be promoted, and migration and invasion can be decreased by activation of ERβ (29). The results of the present study demonstrated that aconitine significantly upregulated the expression of ERβ in A2780 cells, and decreased the expression of HIF-1α and VEGF-A. Therefore, the anticancer effect of aconitine in OVCA cells may result primarily from ERβ activation.

Apoptosis serves important roles in eliminating unwanted or damaged cells in a number of physiological and pathological conditions such as hypoxia and inflammation (48), and the Bcl-2 family contains 2 classes, antiapoptotic members and proapoptotic members (49). Bcl-2 is an antiapoptotic member. Bax, a proapoptotic member, is mainly distributed on the mitochondrial membrane, and the loss of mitochondrial membrane potential is closely related to the release of cytochrome C (46). Increased ERβ and PHD2 can induce apoptosis via adjusting caspase-3 and Bax/Bcl-2 signals *in vitro* and *in vivo* (27). MMPs are a family of zinc-dependent proteinases involved in the degradation of the extracellular matrix and the basement

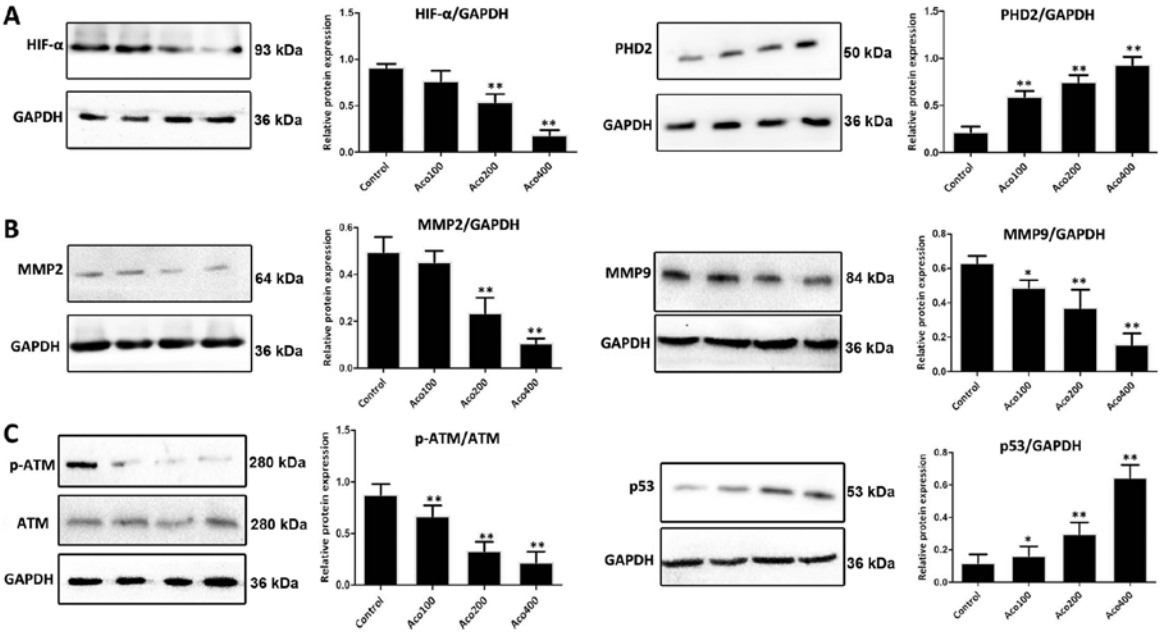

Figure 5. Effects of aconitine on the expression of proteins associated with apoptosis, DNA damage and migration. (A) Effects of aconitine on the expression levels of HIF-α and PHD2. (B) Effects of aconitine on the expression levels of MMP2 and MMP9. (C) Effects of aconitine on the expression levels of ATM, p-ATM and p53. Data are presented as mean ± SD of three independent experiments. *P<0.05, **P<0.01 vs. control group. Aco, aconitine; HIF-α, hypoxia-inducible factor; PHD2, prolyl hydroxylase domain-containing protein 2; MMP, matrix metalloproteinase; ATM, ATM serine/threonine kinase; p-, phosphorylated.

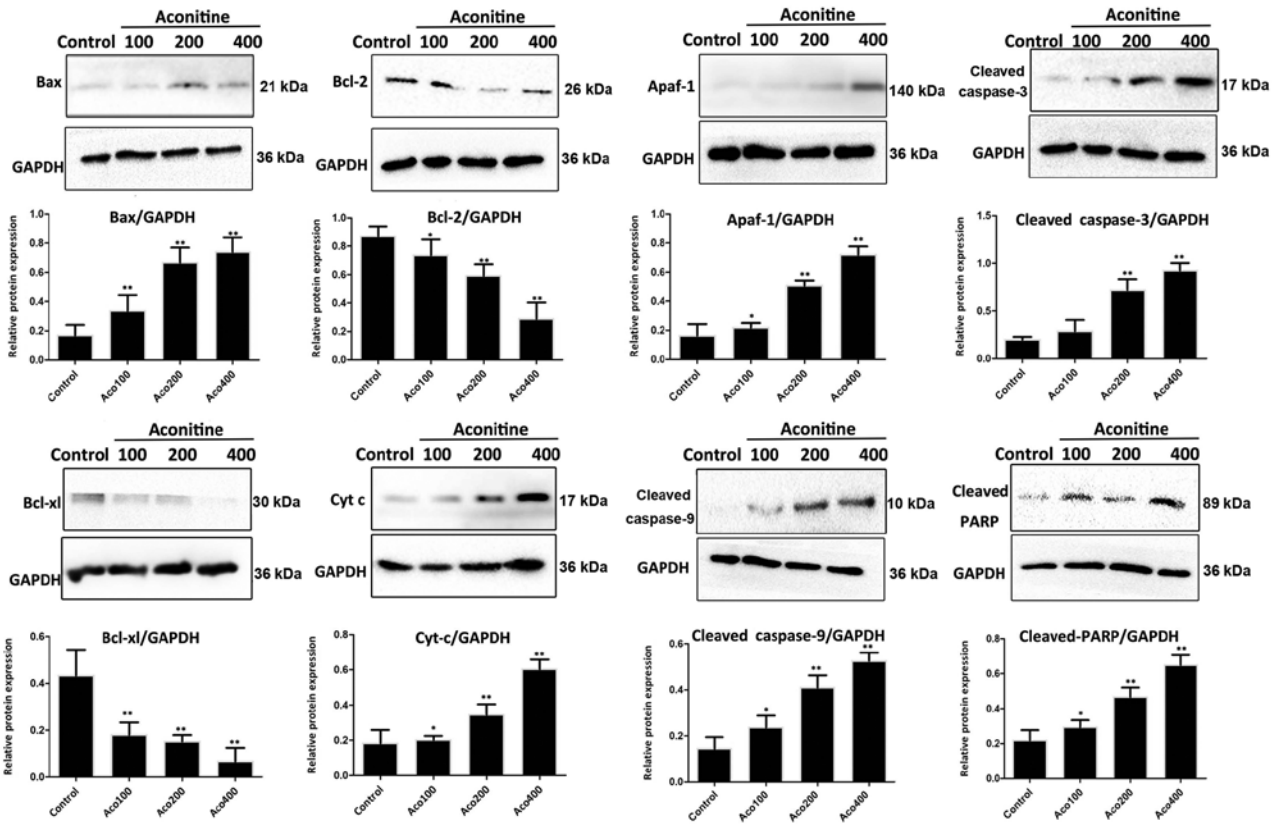

Figure 6. Effects of aconitine on the expression levels of proteins associated with the mitochondria pathway, including Bax, Bcl-2, Apaf-1, cleaved caspase-3, cleaved caspase-9, Bcl-xl, Cyt C and cleaved PARP. Data are presented as mean ± SD of three independent experiments. *P<0.05, **P<0.01 vs. control group. Aco, aconitine; Apaf-1, apoptotic peptidase activating factor 1; Cyt C, cytochrome C; PARP, poly (ADP-ribose) polymerase.

membrane component, and they are associated with the invasion and metastasis of malignant tumors (50). Recent studies have demonstrated that ERβ gene knockdown augments cell proliferation, migration and invasion by regulating cyclin

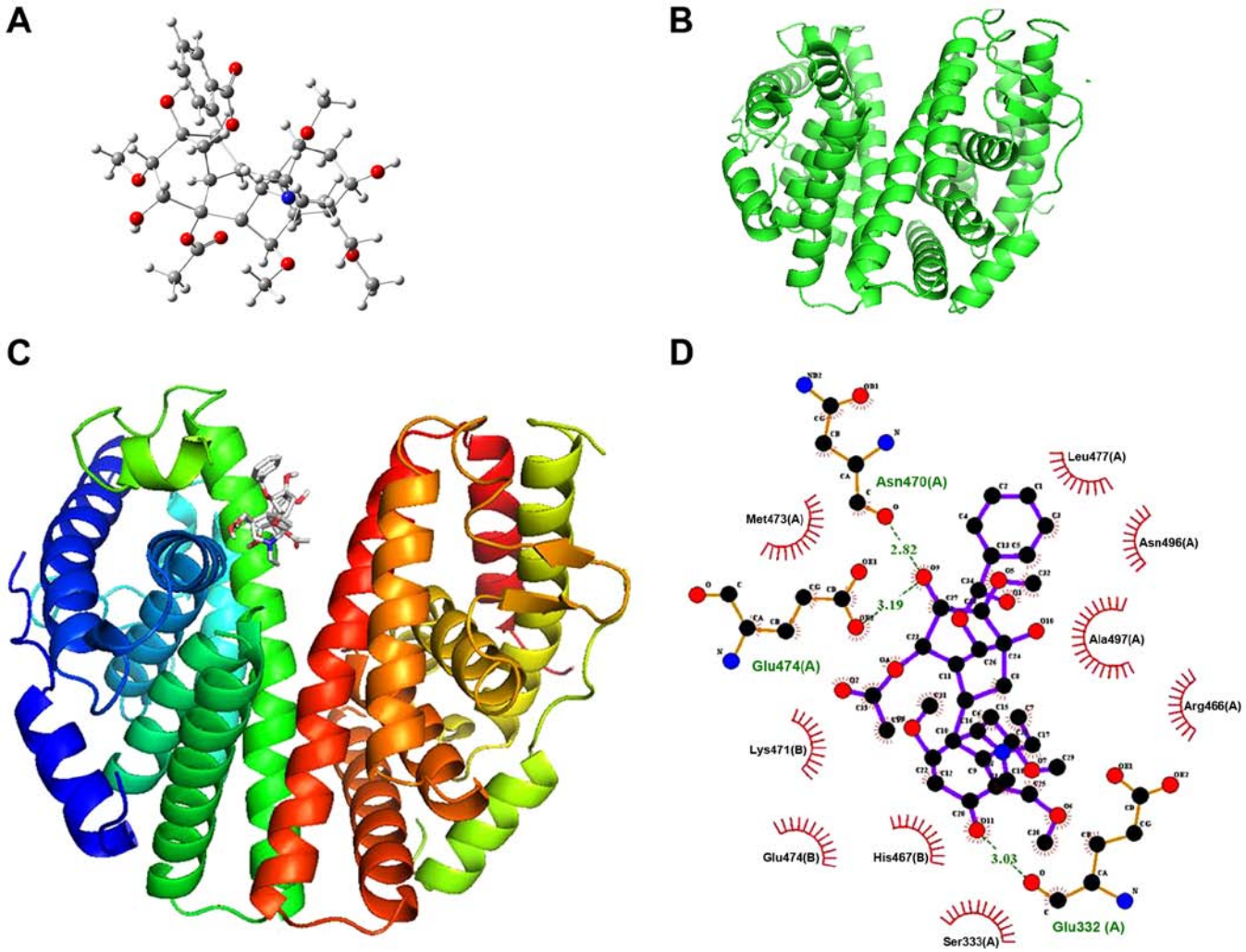

Figure 7. Aconitine directly targets ERβ. (A) 3D structure of aconitine. (B) Crystal structure of ERβ (Protein Data Bank, ID: 2YLY) (C) 3D diagram and (D) schematic diagram of the hydrogen bond interaction between aconitine and ERβ. 3D, three-dimensional; ERβ, estrogen receptor β.

D1 and MMP2 (51). ATM is a serine/threonine kinase that regulates DNA damage by breaking down into active monomers (51). Previous studies revealed that ERβ is required for optimal chemotherapy-induced DNA damage and apoptosis through activation of ATM during the DNA damage response, suggesting that ERβ may function as a tumor suppressor via ATM signaling (52,53). The results of the present study indicated that aconitine decreased the mitochondrial membrane potential and induced mitochondria injury in A2780 cells, and induced apoptosis via adjusting the expression of p53, cytochrome C, cleaved caspases-3/9, Bax/Bcl-2, Bcl-xl, Apaf-1 and cleaved PARP. Notably, the expression levels of MMP2, MMP9 and p-ATM were decreased by aconitine, which may inhibit the development and progression of tumor metastasis and induce DNA damage. In addition, the molecular docking assay results further showed that aconitine possessed powerful affinity towards ERβ, indicating that the compound may directly target the protein for its biological activities. Previously, an ectopic implantation model in nude mice was established to investigate the role of aconitine *in vivo* and the trial suggested that aconitine showed an antimelanoma effect in suppressing tumor growth *in vivo* (54). However, there is no report concerning the antitumor effects of aconitine in OVCA animal models. A previous study has demonstrated that processing (usually boiling) of crude aconite roots decreases the number of toxic alkaloids and increases the concentration of lipo-alkaloids, suggesting that toxic aconite alkaloids cannot be responsible for the anticancer activity, but lipo-alkaloids may be (55). Therefore, in the next study we will work on chemical modification of the drug to decrease the toxicity through lipolyzing in order to make it applicable *in vivo*.

In conclusion, the current study has demonstrated that aconitine decreased cell viability, tumor metastasis and induced apoptosis and DNA damage in A2780 cells via ERβ-mediated signaling (Fig. S2). Further research is required to investigate the mechanisms, drug targets and clinical applications of aconitine against OVCA.

Acknowledgements

Not applicable.

Funding

No funding was received.

Availability of data and materials

The datasets used and/or analyzed during the current study are available from the corresponding author on reasonable request.

Authors' contributions

XW designed the experiments and wrote the manuscript. YL performed data analysis. YZ performed the western blotting assay. XW and YZ edited the manuscript. All authors read and approved the final manuscript.

Ethics approval and consent to participate

Not applicable.

Patient consent for publication

Not applicable.

Competing interests

The authors declare that they have no competing interests.

References

1. Vang R, Shih IM and Kurman RJ: Ovarian Low-grade and High-grade Serous Carcinoma. Pathogenesis clinicopathologic and molecular biologic features and diagnostic problems. Adv Anatomic Pathol 16: 267-282, 2009.
2. Liu J, Zhang Z, Guo Q, Dong Y, Zhao Q and Ma X: Syringin prevents bone loss in ovariectomized mice via TRAF6 mediated inhibition of NF-κB and stimulation of PI3K/AKT. Phytomedicine 42: 43-50, 2018.
3. Han CY, Patten DA, Richardson RB, Harper ME and Tsang BK: Tumor metabolism regulating chemosensitivity in ovarian cancer. Genes Cancer 9: 155-175, 2018.
4. Hainsworth JD, Thompson DS, Bismayer JA, Gian VG, Merritt WM, Whorf RC Finney LH and Dudley BS: Paclitaxel/carboplatin with or without sorafenib in the first-line treatment of patients with stage III/IV epithelial ovarian cancer: A randomized phase II study of the Sarah Cannon Research Institute. Cancer Med 4: 673-681, 2015.
5. Wilhelm SM, Carter C, Tang L, Wilkie D, McNabola A, Rong H, Chen C, Zhang X, Vincent P, McHugh M, *et al*: BAY 43-9006 exhibits broad spectrum oral antitumor activity and targets the RAF/MEK/ERK pathway and receptor tyrosine kinases involved in tumor progression and angiogenesis. Cancer Res 64: 7099-7109, 2004.
6. Treeck O, Lattrich C, Springwald A and Ortmann O: Estrogen receptor beta exerts growth-inhibitory effects on human mammary epithelial cells. Breast Cancer Res Treat 120: 557-565, 2010.
7. Treeck O, Juhasz-Boess I, Lattrich C, Horn F, Goerse R and Ortmann O: Effects of exon-deleted estrogen receptor beta transcript variants on growth, apoptosis and gene expression of human breast cancer cell lines. Breast Cancer Res Treat 110: 507-520, 2008.
8. Chan KKL, Siu MKY, Jiang YX, Wang JJ, Leung THY and Ngan HYS: Estrogen receptor modulators genistein, daidzein and ERB-041 inhibit cell migration, invasion, proliferation and sphere formation via modulation of FAK and PI3K/AKT signaling in ovarian cancer. Cancer Cell Int 18: 65, 2018.
9. Leung YK, Mak P, Hassan S and Ho SM: Estrogen receptor (ER)-beta isoforms: A key to understanding ER-beta signaling. Proc Natl Acad Sci USA 103: 13162-13167, 2006.
10. Schuler-Toprak S, Weber F, Skrzypczak M, Ortmann O and Treeck O: Estrogen receptor beta is associated with expression of cancer associated genes and survival in ovarian cancer. BMC Cancer 18: 981, 2018.
11. Mak P, Leav I, Pursell B, Bae D, Yang X, Taglienti CA, Gouvin LM, Sharma VM and Mercurio AM: ERbeta impedes prostate cancer EMT by destabilizing HIF-1alpha and inhibiting VEGF-mediated snail nuclear localization: Implications for Gleason grading. Cancer Cell 17: 319-332, 2010.
12. Wang Y, Niu XL, Guo XQ, Yang J, Li L, Qu Y, Xiu Hu C, Mao LQ and Wang D: IL6 induces TAM resistance via kinase-specific phosphorylation of ERα in OVCA cells. J Mol Endocrinol 54: 351-361, 2015.
13. Halon A, Nowak-Markwitz E, Maciejczyk A, Pudelko M, Gansukh T, Györffy B, Donizy P, Murawa D, Matkowski R, Spaczynski M, *et al*: Loss of estrogen receptor beta expression correlates with shorter overall survival and lack of clinical response to chemotherapy in ovarian cancer patients. Anticancer Res 31: 711-718, 2011.
14. Fixemer T, Remberger K and Bonkhoff H: Differential expression of the estrogen receptor beta (ER beta) in human prostate tissue, premalignant changes, and in primary, metastatic, and recurrent prostatic adenocarcinoma. Prostate 54: 79-87, 2003.
15. Mak P, Chang C, Pursell B and Mercurio AM: Estrogen receptor βsustains epithelial differentiation by regulating prolyl hydroxylase 2 transcription. Proc Natl Acad Sci USA 110: 4708-4713, 2013.
16. Goel HL and Mercurio AM: VEGF targets the tumour cell. Nat Rev Cancer 13: 871-882, 2013.
17. Bhattacharya R, Ye XC, Wang R, Ling X, McManus M, Fan F, Boulbes D and Ellis LM: Intracrine VEGF signaling mediates the activity of prosurvival pathways in human colorectal cancer cells. Cancer Res 76: 3014 3024, 2016.
18. Wang ZY, Zarlenga D, Martin J, Abubucker S and Mitreva M: Exploring metazoan evolution through dynamic and holistic changes in protein families and domains. BMC Evolut Biol 12: 138, 2012.
19. Xu GL, Xie M, Yang XY, Song Y, Yan C, Yang Y, Zhang X, Liu ZZ, Tian YX, Wang Y, *et al*: Spectrum-effect relationships as a systematic approach to traditional chinese medicine research: Current status and future perspectives. Molecules 19: 17897-17925, 2014.
20. Xu J and Yang Y: Traditional Chinese medicine in the Chinese health care system. Health Policy 90: 133-139, 2009.
21. Wang S, Wu X, Tan M, Gong J, Tan W, Bian B, Chen M and Wang Y: Fighting fire with fire: Poisonous Chinese herbal medicine for cancer therapy. J Ethnopharmacol 140: 33-45, 2012.
22. Lv L, Zheng L, Dong D, Xu L, Yin L, Xu Y, Qi Y, Han X and Peng J: Dioscin, a natural steroid saponin, induces apoptosis and DNA damage through reactive oxygen species: A potential new drug for treatment of glioblastoma multiforme. Food Chem Toxicol 59: 657-669, 2013.
23. Zhao X, Xu L, Zheng L, Yin L, Qi Y, Han X, Xu Y and Peng J: Potent effects of dioscin against gastric cancer in vitro and in vivo. Phytomedicine 23: 274-282, 2016.
24. Si L, Zheng L, Xu L, Yin L Han X, Qi Y, Xu Y, Wang C and Peng J: Dioscin suppresses human laryngeal cancer cells growth via induction of cell-cycle arrest and MAPK-mediated mitochondrial derived apoptosis and inhibition of tumor invasion. Eur J Pharmacol 774: 105-117, 2016.
25. Si L, Xu L, Yin L, Qi Y, Han X, Xu Y, Zhao Y, Liu K and Peng J: Potent effects of dioscin against pancreatic cancer via miR-149-3P-mediated inhibition of the AKT1 signaling pathway. Br J Pharmacol 174: 553-568, 2017.
26. Mao Z, Han X, Chen D, Xu Y, Xu L, Yin L, Sun H, Qi Y, Fang L, Liu K and Peng J: Potent effects of dioscin against hepatocellular carcinoma through regulating TIGAR-mediated apoptosis, autophagy and DNA damage. Br J Pharmacol 176: 919-937, 2019.
27. Tao X, Xu L, Yin L, Han X, Qi Y, Xu Y, Song S, Zhao Y and Peng J: Dioscin induces prostate cancer cell apoptosis through activation of Estrogen Receptor-β. Cell Death Dis 8: e2989, 2017.
28. Chen H, Xu L, Yin L, Xu Y, Han X, Qi Y and Peng J: iTRAQ-based proteomic analysis of dioscin on human HCT-116 colon cancer cells. Proteomics 14: 51-73, 2014.
29. Lu B, Hu M, Liu K and Peng J: Cytotoxicity of berberine on human cervical carcinoma HeLa cells through mitochondria, death receptor and MAPK pathways, and in-silico drug-target prediction. Toxicol in Vitro 24: 1482-1490, 2010.
30. Wei Y, Xu YS, Han X, Qi Y, Xu L, Xu Y, Yin L, Sun H, Liu K and Peng J: Anti-cancer effects of dioscin on three kinds of human lung cancer cell lines through inducing DNA damage and activating mitochondrial signal pathway. Food Chem Toxicol 59: 118-128, 2013.

31. Ning Y, Feng W, Cao X, Ren K, Quan M, Chen A, Xu C, Qiu Y, Cao J, Li X and Luo X: Genistein inhibits stemness of SKOV3 cells induced by macrophages co-cultured with ovarian cancer stem-like cells through IL-8/STAT3 axis. J Exp Clin Cancer Res 38: 19, 2019.
32. Wang MY, Liang JW, Olounfeh KM, Sun Q, Zhao N and Meng FH: A comprehensive in silico method to study the QSTR of the aconitine alkaloids for designing novel drugs. Molecules 23: pii: E2385, 2018.
33. Ji BL, Xia LP, Zhou FX, Mao GZ and Xu LX: Aconitine induces cell apoptosis in human pancreatic cancer via NF-κB signaling pathway. Eur Rev Med Pharmacol Sci 20: 4955-4964, 2016.
34. Li XM, Liu J, Pan FF, Shi DD, Wen ZG and Yang PL: Quercetin and aconitine synergistically induces the human cervical carcinoma HeLa cell apoptosis via endoplasmic reticulum (ER) stress pathway. PLoS One 13: e0191062, 2018.
35. Frisch M, Trucks G, Schlegel H, Scuseria G, Robb M, Heeseman J, Scalmani G, Barone V, Petersson GA, Nakatsuji H, *et al*: Gaussian 09, Revision A.02. Gaussian, Inc., Wallingford CT, 2009.
36. Becke A: Density-functional thermochemistry. III. The role of exact exchange. J Chem Phys 98: 5648-5653, 1993.
37. Lee C, Yang W and Parr R: Development of the colic-salvetti correlation-energy formula into a functional of the electron density. Phys Rev B Condens Matter 37: 785-789, 1988.
38. Schüttelkopf AW and Van Aalten DM: PRODRG: A tool for high-throughput crystallography of protein-ligand complexes. Acta Crystallogr D Biol Crystallogr 60: 1355-1363, 2004.
39. Zhang S, Leng T, Zhang Q, Zhao Q, Nie X and Yang L: Sanguinarine inhibits epithelial ovarian cancer development via regulating long non-coding RNA CASC2- EIF4A3 axis and/or inhibiting NF-κB signaling or PI3K/AKT/mTOR pathway. Biomed Pharmacother 102: 302-308, 2018.
40. Zhu L, Liu X, Li D, Sun S, Wang Y and Sun X: Autophagy is a pro-survival mechanism in ovarian cancer against the apoptotic effects of euxanthone. Biomed Pharmacother 103: 708-718, 2018.
41. Xia Z, Lundgren B, Bergstrand A, DePierre JW and Nässberger L: Changes in the generation of reactive oxygen species and in mitochon- drial membrane potential during apoptosis induced by the antidepressant imipramine, clomipramine, and citalopram and the effects on these changes by Bcl-2 and Bcl-X(L). Biochem Pharmacol 57: 1199-1208, 1999.
42. Wang X: The expanding role of mitochondria in apoptosis. Genes Dev 15: 2922-2933, 2001.
43. Li Z, Fan EK, Liu J, Scott MJ, Li Y, Li S, Xie W, Billiar TR, Wilson MA, Jiang Y, *et al*: Cold-inducible RNA-binding protein through TLR4 signaling induces mitochondrial DNA fragmentation and regulates macrophage cell death after trauma. Cell Death Dis 8: e2775, 2017.
44. Anestis A, Sarantis P, Theocharis S, Zoi I, Tryfonopoulos D, Korogiannos A, Koumarianou A, Xingi E, Thomaidou D, Kontos M, *et al*: Estrogen receptor beta increases sensitivity to enzalutamide in androgen receptor-positive triple-negative breast cancer. J Cancer Res Clin Oncol 145: 1221-1233, 2019.
45. Foley EF, Jazaeri AA, Shupnik MA, Jazaeri O and Rice LW: Selective loss of estrogen receptor beta in malignant human colon. Cancer Res 60: 245-248, 2000.
46. Rutherford T, Brown WD, Sapi E, Aschkenazi S, Muñoz A and Mor G: Absence of estrogen receptor-beta expression in metastatic ovarian cancer. Obstet Gynecol 96: 417-421, 2000.
47. Zimmermann KC and Green DR: How cells die: Apoptosis pathways. J Allergy Clin Immunol 108: 99-103, 2001.
48. Iakova P, Timchenko L and Timchenko NA: Intracellular signaling and hepatocellular carcinoma. Semin Cancer Biol 21: 28-34, 2011.
49. Liu J, Yin S, Reddy N, Spencer C and Sheng S: Bax mediates the apoptosis-sensitizing effect of maspin. Cancer Res 64: 1703-1711, 2004,
50. Sarig-Nadir O and Seliktar D: The role of matrix metalloproteinases in regulating neuronal and nonneuronal cell invasion into PEGylated fibrinogen hydrogels. Biomaterials 31: 6411-6416, 2010.
51. Zhao Z, Yu H and Kong Q: Effect of ERβ-regulated ERK1/2 signaling on biological behaviors of prostate cancer cells. Am J Transl Res 9: 2775-2787, 2017.
52. Peng M, Yang D, Hou Y, Liu S, Zhao M, Qin Y, Chen R, Teng Y and Liu M: Intracellular citrate accumulation by oxidized ATM-mediated metabolism reprogramming via PFKP and CS enhances hypoxic breast cancer cell invasion and metastasis. Cell Death Dis 10: 228, 2019.
53. Zhou M, Sareddy GR, Li M, Liu J, Luo Y, Venkata PP, Viswanadhapalli S, Tekmal RR, Brenner A and Vadlamudi RK: Estrogen receptor beta enhances chemotherapy response of GBM cells by down regulating DNA damage response pathways. Sci Rep 9: 6124, 2019.
54. Du J, Lu X, Long Z, Zhang Z, Zhu X, Yang Y and Xu J: In vitro and in vivo anticancer activity of aconitine on melanoma cell line B16. Molecules 18: 757-767, 2013.
55. Borcsa B, Widowitz U, Csupor D, Forgo P, Bauer R and Hohmann J: Semisynthesis and pharmacological investigation of lipo-alkaloids prepared from aconitine. Fitoterapia 82: 365-368, 2011.